The Journal of Experimental Biology 214, 1357-1368

doi:10.1242/jeb.051169

RESEARCH ARTICLE

Early development and molecular plasticity in the Mediterranean sea urchin *Paracentrotus lividus* exposed to CO_2-driven acidification

Sophie Martin[1,2,3,*], Sophie Richier[4,5], Maria-Luiza Pedrotti[4,5], Sam Dupont[6], Charlotte Castejon[1], Yannis Gerakis[4,5], Marie-Emmanuelle Kerros[4,5], François Oberhänsli[1], Jean-Louis Teyssié[1], Ross Jeffree[1,†] and Jean-Pierre Gattuso[4,5]

[1]Marine Environment Laboratories, International Atomic Energy Agency, 4 Quai Antoine I[er], 98000 Principality of Monaco, [2]CNRS, Laboratoire Adaptation et Diversité en Milieu Marin, Station Biologique de Roscoff, Place Georges Teissier, 29682 Roscoff Cedex, France, [3]Université Pierre et Marie Curie, Paris 06, Laboratoire Adaptation et Diversité en Milieu Marin, Station Biologique de Roscoff, Place Georges Teissier, 29682 Roscoff Cedex, France, [4]CNRS-INSU, Laboratoire d'Océanographie de Villefranche-sur-Mer, BP 28, 06234 Villefranche-sur-Mer Cedex, France, [5]Université Pierre et Marie Curie, Paris 06, Observatoire Océanologique de Villefranche, 06230 Villefranche-sur-Mer Cedex, France and [6]Department of Marine Ecology, University of Göteborg, The Sven Lovén Centre for Marine Science, Kristineberg, 45034 Fiskebäckskil, Sweden

*Author for correspondence (sophie.martin@sb-roscoff.fr)

†Present address: Faculty of Science, University of Technology, Sydney, P.O. Box 123, Broadway, NSW 2007, Australia

Accepted 5 January 2011

SUMMARY

Ocean acidification is predicted to have significant effects on benthic calcifying invertebrates, in particular on their early developmental stages. Echinoderm larvae could be particularly vulnerable to decreased pH, with major consequences for adult populations. The objective of this study was to understand how ocean acidification would affect the initial life stages of the sea urchin *Paracentrotus lividus*, a common species that is widely distributed in the Mediterranean Sea and the NE Atlantic. The effects of decreased pH (elevated P_{CO_2}) were investigated through physiological and molecular analyses on both embryonic and larval stages. Eggs and larvae were reared in Mediterranean seawater at six pH levels, i.e. pH_T 8.1, 7.9, 7.7, 7.5, 7.25 and 7.0. Fertilization success, survival, growth and calcification rates were monitored over a 3 day period. The expression of genes coding for key proteins involved in development and biomineralization was also monitored. *Paracentrotus lividus* appears to be extremely resistant to low pH, with no effect on fertilization success or larval survival. Larval growth was slowed when exposed to low pH but with no direct impact on relative larval morphology or calcification down to pH_T 7.25. Consequently, at a given time, larvae exposed to low pH were present at a normal but delayed larval stage. More surprisingly, candidate genes involved in development and biomineralization were upregulated by factors of up to 26 at low pH. Our results revealed plasticity at the gene expression level that allows a normal, but delayed, development under low pH conditions.

Key words: early life stage, sea urchin, development, calcification, gene expression, ocean acidification.

INTRODUCTION

Atmospheric CO_2 concentrations have risen from a preindustrial value of ~280 ppm to a current value of 387 ppm because of human activities (Solomon et al., 2007). Simulation models project that concentrations could reach 1200 ppm by the end of this century and nearly 2000 ppm by approximately 2300 (Caldeira and Wickett, 2003; Caldeira and Wickett, 2005). Diffusion of atmospheric CO_2 in the surface ocean causes an increase in the partial pressure of CO_2 (P_{CO_2}) and is likely to decrease pH by 0.2–0.4 units over the course of this century and by up to 0.77 units by 2300 (Caldeira and Wickett, 2003; Caldeira and Wickett, 2005; Turley et al., 2009). Such a decline in pH of surface waters will reduce carbonate ion (CO_3^{2-}) concentrations and the degree of calcium carbonate ($CaCO_3$) saturation in seawater, which could negatively affect marine organisms that synthesize a carbonate skeleton. Exposure to high CO_2 levels and subsequent lowered pH may have biological consequences for juveniles and adults of different groups of benthic calcifying organisms such as corals (Gattuso et al., 1999; Anthony et al., 2008; Suwa et al., 2010), mollusks (Green et al., 2004; Berge et al., 2006; Gazeau et al., 2007; Kurihara et al., 2007) and echinoderms (Shirayama and Thornton, 2005; Miles et al., 2007; Gooding et al., 2009; Dupont et al., 2010a). The life cycle of many of these animals comprises a planktonic larval phase. Although embryos and larvae are well prepared for environmental changes (Hamdoun and Epel, 2007), it is widely accepted that early life-history stages are more sensitive than adults to ocean acidification (Raven et al., 2005; Pörtner and Farrell, 2008; Dupont et al., 2010b). Previous investigations on echinoderms have demonstrated a decrease in fertilization and larval survival rates, developmental speed and size, and an increase in malformed skeletogenesis with decreasing pH (reviewed in Dupont et al., 2010c). Recent studies, performed at a molecular level in sea urchin larvae, revealed that genes involved in several biological processes undergo broad-scale decreases in expression at elevated CO_2 levels (Todgham and Hofmann, 2009; O'Donnell et al., 2010). However, these differences were observed at one time point and may be partially explained by a delay in the development classically observed under low pH conditions (Pörtner et al., 2010).

Among these studies, several examined the effects of pH levels predicted for this century (from 8.1 to 7.6) whereas others determined pH thresholds for larval development and survival down to pH levels (from 7.5 to 6.0) far below those predicted for this century. It is thus not possible at this stage to conclude that the first life stages of benthic invertebrates will respond negatively to ocean acidification in the near future. In addition, within a range applicable to climate change scenarios, results are very disparate depending on species, their life-history stage and the biological parameters tested (Dupont et al., 2010b; Dupont et al., 2010c). In the Echinodermata, the early life stage development of some brittlestar (Dupont et al., 2008) or sea urchin species (Havenhand et al., 2008; Clark et al., 2009; Reuter et al., 2010) is slowed or even completely disrupted at pH levels predicted for the end of this century whereas there may be a broad tolerance to such pH levels in other species of sea urchins (Kurihara and Shirayama, 2004; Byrne et al., 2009a; Byrne et al., 2009b; Byrne et al., 2010; Clark et al., 2009), with even some positive effects observed in lecithotropic seastars (Dupont et al., 2010a). The larval stage of many echinoderms is planktonic and comprises a critical period in their life cycle because recruitment success is primarily determined by the survival of embryos and larvae (McEdward and Miner, 2007). Therefore, any decrease in the larval survival rates and settlement success may well reduce the long-term viability of affected populations. Consequently, more data on the response of larval stages to ocean acidification are required to understand its impact on biological processes that are essential for the integrity and persistence of these populations.

In the present study, we explored the effect of a gradient of decreasing pH from 8.1 to 7.0 on the larvae of the sea urchin *Paracentrotus lividus* (Lamarck 1816), a common species that is widely distributed throughout the Mediterranean Sea and the NE Atlantic from Ireland to southern Morocco. This species is both economically and ecologically important, especially in the Mediterranean Sea where it provides the largest economic return for sea urchin fisheries. It also acts as a keystone species, being the dominant grazer in the majority of shallow Mediterranean benthic communities, which are composed of rocks and boulders, coralligenous concretions or seagrass meadows that extend from the low-water limit down to ~20 m depth (Boudouresque and Verlaque, 2001). Larvae are produced during well-defined periods and remain in the superficial layer until metamorphosis. Therefore, any change affecting survival or growth reduces the number of individuals recruited and leads to major changes in Mediterranean ecosystems (Pedrotti and Fenaux, 1992).

This study used multiple methods to identify the response of *P. lividus* to CO_2-driven ocean acidification at both physiological (fertilization, growth, survival and calcification) and molecular (expression of genes involved in calcification and development) levels.

MATERIALS AND METHODS

Biological material and experimental procedures

Specimens of the sea urchin *P. lividus* were collected by SCUBA divers from subtidal rocky shores at *ca*. 10 m depth in the vicinity of the Laboratoire d'Océanographie de Villefranche in the Bay of Villefranche (NW Mediterranean Sea, France) in March and April 2009, at the beginning of the period of gonadal maturity in this species. The reproductive cycle of *P. lividus* in the Mediterranean Sea consists of two spawning events: a small one in late spring and a second one in late summer (Fenaux, 1968). In the Bay of Villefranche, the main spawning event occurs from mid-May to July (Fenaux et al., 1987), with recruitment at the end of spring and at the end of summer. Sea urchins were maintained in flowing unfiltered Mediterranean seawater (salinity 38) pumped from 10 m depth in the Bay of Villefranche and fed with *Posidonia oceanica* blades. Sea urchins were opened around the peristome to obtain ripe gonadal material from one male and three females. To collect eggs, female gonads were placed on a 200 μm mesh nylon filter above a beaker and rinsed three times with filtered (0.22 μm) Mediterranean seawater (FSW; salinity 38). The eggs were washed three times by sedimentation and resuspension in FSW. Eggs from the three females were then pooled. Sperm was collected dry using a Pasteur pipette, transferred to a small tube and stored at 4°C pending fertilization. After collection (maximum 1 h), eggs and sperm were transferred to the Radioecology Laboratory (Marine Environment Laboratories of the International Atomic Energy Agency, Monaco) for fertilization. The eggs were concentrated by removing the supernatant seawater. The density of the egg suspension was determined from 0.1 ml subsamples by counting eggs under a binocular microscope. Aliquots of egg suspension (180,000 eggs, *ca*. 50 ml) were transferred to 1 l beakers filled with FSW previously adjusted to the desired pH and temperature levels (see below) and labelled with ^{45}Ca (experiment A) or kept radiotracer-free (experiment B). Sperm was diluted 1:50 in FSW and 5 ml of this dilution was added to the egg suspension. Eggs were gently agitated for 15 min to optimize fertilization and then were transferred to 4.5 l beakers filled with labelled or radiotracer-free FSW. The FSW was gently aerated and maintained in controlled conditions of temperature and pH (see below). The experiment was conducted from Day 0 (fertilization) to Day 3 (feeding four-arm stage). A volume of 1.5 to 2 l seawater was collected daily for Ca incorporation or gene expression analyses and replaced by new FSW. The larval density changed according to the dilution of the culture because of seawater sampling and decreased from 35 individuals ml^{-1} at Day 0 to 12 individuals ml^{-1} at Day 3 in experiment A and from 32 to 11 individuals ml^{-1} in experiment B.

Experimental setup and carbonate chemistry measurements

For each experiment, 4.5 l beakers were placed in a 300 l bath kept at a constant temperature of 20°C, which is the optimal growth temperature for larvae of *P. lividus* (Pedrotti and Fenaux, 1993). Temperature was controlled to within ±0.5°C using a temperature controller (IKS, Karlsbad, Germany) connected to 300 W submersible heaters. Seawater pH (pH_T, expressed on the total hydrogen ion concentration scale, which is recommended for use in characterising the pH of seawater) (Dickson, 2010) was adjusted to the desired level from ambient pH_T (8.1) to low pH_T (7.9, 7.7, and 7.5) conditions as derived from various IPCC models on trajectories of carbon emissions to the year 2100 (Orr et al., 2005). Two lower pH_T conditions (7.25 and 7.0) were also tested. pH_T was controlled in each beaker to within ±0.05 pH units using a continuous pH-stat system (IKS) that controlled the addition of CO_2 into the beakers, which were continuously aerated with CO_2-free air. The pH values of the pH-stat system were adjusted from measurements of pH_T in each beaker using a pH meter (Metrohm 826 pH mobile, Metrohm, Herisau, Switzerland) with a glass electrode (Metrohm electrode plus) calibrated on the total scale using Tris/HCl and 2-aminopyridine/HCl buffer solutions prepared in synthetic seawater with a salinity of 38 according to Dickson et al. (Dickson et al., 2007). Total alkalinity (A_T) shifts from the beginning to the end of the experiment were assessed in seawater from the beakers maintained in the free-radiotracer laboratory (experiment B). A_T was measured on seawater samples filtered through 0.45 μm membranes, immediately poisoned with mercuric chloride and stored in a cool

dark place pending analyses. A_T was determined potentiometrically using a laboratory-constructed titration system with an Orion 8103SC pH electrode (Orion Research Inc., Boston, MA, USA) calibrated on the National Bureau of Standards scale and a computer-driven Metrohm 665 Dosimat titrator. A_T was calculated using a Gran function applied to pH values ranging from 3.5 to 3.0 as described by Dickson et al. (Dickson et al., 2007). Titrations of an A_T standard provided by A. G. Dickson (batch 95) were within 0.6 µmol kg^{-1} of the nominal value (s.d.=1.3 µmol kg^{-1}; N=5). The partial pressure of CO_2 (P_{CO_2}) and other parameters of carbonate chemistry were determined from pH and total alkalinity using the R package seacarb (Lavigne and Gattuso, 2010). The saturation state of both calcite (Ω_c) and aragonite (Ω_a) were used to assess mineral availability because the saturation state of echinoderm high magnesium calcite is still under debate, but is likely to be close to aragonite (Morse et al., 2007).

Measurements of fertilization, survival and development

Fertilization success was determined after 2 h as the proportion of eggs that had a fertilization envelope or exhibited cleavage. The number of fertilized eggs was counted on six replicate 1 ml subsamples taken from each beaker in experiments A and B. Density was measured daily on six replicate 1 ml subsamples. Larval survival (S_t, %) was calculated from the density at time t (N_t, larvae ml^{-1}) and a dilution factor (d) determined according to the volume of sampled and renewed seawater as: $S_t=100\times N_t/(N_{t-1}\times d)$. Samples of larvae (5–30 ml) were collected on Day 2 (t=46 and 52 h post-fertilization) and Day 3 (t=69 h post-fertilization). They were fixed with buffered 4% formaldehyde for examination by microscopy. To distinguish the larvae, the samples were stained with Rose Bengal, filtered on 0.4 µm polycarbonate membrane, mounted on slides in glycerol and measured under optical microscopy. The larval overall length (somatic rod + post-oral arm) was measured from Day 2 (46 h) to Day 3 (69 h). The lengths of somatic rods, post-oral arms and antero-lateral arms and the width of larvae were measured on Day 3. Ratios of the left to right overall length (symmetry index) and of the post-oral arm to somatic rod length were calculated on Day 3. The former was used as an indicator of the entrance of larvae in the exotrophic phase; a ratio higher than 1 indicates start-feeding larvae (Bougis, 1971). Data were analysed using one- and two-way ANOVAs. Data transformation was performed when conditions of normal distribution and homogeneity of variance were not met. Tukey's honestly significant difference (HSD) multiple comparison tests were carried out to assess the significance of differences between groups. Morphometric parameters (somatic rod, post-oral arm and antero-lateral arm lengths and larval width) were related to overall length using linear relationships. Analyses of covariance (ANCOVAs) were performed to test for differences between intercepts and slopes. Pairwise ANCOVAs were conducted to test significant differences between pairs of pH treatments.

Measurements of ^{45}Ca uptake

For determination of embryonic and larval Ca uptake, eggs were incubated in seawater labelled with 50 kBq l^{-1} ^{45}Ca as $^{45}CaCl_2$ (specific activity=1093.06 MBq mg^{-1}; PerkinElmer Life and Analytical Sciences, Inc., Boston, MA, USA). Seawater was spiked before the addition of eggs and sperm and 5 ml seawater samples were collected from each pH treatment for radioactivity counting. Seawater samples of 250 to 400 ml (depending on the culture concentration) were collected at Day 0 (t=5 h post-fertilization), Day 1 (t=20, 23 and 27 h post-fertilization), Day 2 (t=46 and 53 h post-fertilization) and Day 3 (t=76 h post-fertilization). Day 1 (27 h) and Days 2 and 3 were sampled in triplicate. Larvae were filtered through a 20 µm polycarbonate membrane, resuspended and rinsed three times in radiotracer-free FSW. Before resuspension and rinsing, 5 ml of seawater were sampled in the filtrate for radioactivity counting. The filters were transferred to 20 ml glass scintillation counting vials and digested with nitric acid at 50°C. After digestion, the samples were dried at 60°C until complete acid evaporation and were resuspended in 1 ml distilled water. Seawater and filter samples were counted for 1 h in a liquid scintillation β counter (Tricarb 2900 TR, PerkinElmer) after the addition of 10 ml scintillation liquid (Ultima Gold XR, PerkinElmer). Radioactivity in seawater, embryos and larvae was measured in counts per minute (CPM). CPM were corrected for quenching and converted to Bq (1 Bq= 1 disintegration s^{-1}). Quenching curves (relationship between quench parameter and counting efficiency) were established for seawater, embryos and larvae by counting sets of 10 samples with the same activity but with variable quantities of seawater, eggs or larvae. The amount of Ca incorporated (Q_{Ca}, in nmol Ca individual^{-1}) was calculated according to:

$$Q_{Ca} = \{[(A_{su} / N_{su}) / A'_{sw}] \times C_{sw}\} \times 10^6, \quad (1)$$

where A_{su} is the total ^{45}Ca activity in sea urchin embryos (or larvae, in Bq), N_{su} is the number of sea urchin embryos (or larvae), A'_{sw} is the time-integrated activity (in Bq g^{-1}) in seawater during the time of exposure and C_{sw} is the total Ca concentration in Mediterranean seawater (0.0114 mmol g^{-1}). Adsorption of ^{45}Ca on filters was checked using a control 4.5 l beaker without organisms that was filled with FSW labelled with 50 kBq l^{-1} ^{45}Ca. The total activity in the filters was determined according to the procedure previously described. Passive ^{45}Ca adsorption on tissues was also tested using dead embryos incubated for 2 days in FSW labelled with 50 kBq l^{-1} ^{45}Ca. Spearman's rank correlation (r_S) was used to test the effect of lowering pH on Ca incorporation. ANCOVAs were performed to test heterogeneity of slopes among pH treatments. Pairwise ANCOVAs were conducted to test significant differences between pairs of treatments.

Measurements of gene expression

RNA extraction

Seawater samples from 300 to 750 ml (depending on the culture concentration) were collected in triplicate on Day 1 (t=22 h post-fertilization), Day 2 (t=46 and 52 h post-fertilization) and Day 3 (t=69 h post-fertilization). The larvae were filtered through a 20 µm polycarbonate membrane and stored at –80°C pending RNA analysis. Total RNA was extracted from ~8500 larvae in 1 ml of Trizol reagent (Invitrogen, La Jolla, CA, USA) according to the manufacturer's suggested protocol. Two successive chloroform (≥99%) steps in 200 µl were carried out to precipitate proteins and DNA. RNA was finally precipitated in 500 µl isopropanol (≥99%). The pellets were washed in 75% ethanol and resuspended in sterile water. The RNA quality was checked on 1% agarose (w/v) gel and presented sharp ribosomal RNA bands with a 28S/18S ratio of 2:1. RNA samples were treated with DNAse (1 U µl^{-1}; Fermentas, Saint-Remy-les-Chevreuse, France) and quantified using a RiboGreen RNA Quantification Kit (Molecular Probes, Cergy Pontoise, France). The total RNA concentration was adjusted to a final concentration of 100 ng µl^{-1} in all samples and reverse transcription was carried out using the Affinity Script qPCR cDNA kit (Agilent Technologies, Massy, France). RNAsin (1 µl, recombinant RNAsin, ribonuclease inhibitor, Promega) was added to each cDNA synthesis mix to avoid further degradation of the template. Negative controls

Table 1. Transcripts targeted in the experiments, length of the amplified product (bp) and primer sequences

Protein	Gene ID	Primer name	Primer sequence	Amplicon length (bp)
Polyubiquitin	AM596937.1	Pl_polyubi F Pl_polyubi R	TCCGTGGTGGTCAATAGAGT ATGGGTGCATTTGCTCTTG	158
SM30	AM569342.1	Pl_SM30 F Pl_SM30 R	GAGAAACAACCCTGCTCCTT TCGGTTCATCCTGTAGTTGG	109
msp130	AM568814	Pl_msp130 F1 Pl_msp130 R1	ATACATGGCAACCCAAGAAG CGATTCCAACGAAGATGAGT	130
α-Na^+/K^+/ATPase	AM562805.1	Pl_NaKATPa F1 Pl_NaKATPa R	AGGCTTGCGTCTTCTTGATT TTCTTCACCAGGCAGTTCTT	123
β-Na^+/K^+/ATPase	AM554663.1	Pl_NaKATPb F Pl_NaKATPb R1	CTGGACGCAGTATGGGATT AATGCAAGGCTCTGTTGTGT	180
Fibroblast growth factor (fg9/16/20)	ABO65253	Pl_fgf9/16/20 F1 Pl_fgf9/16/20 R1	GCCAGCTCTACGTCTGTGTT CTGGACTCGCCGTACTTATT	196

(same reagents mix without reverse transcriptase) were prepared simultaneously and run on each plate for each primer pair to ascertain that no DNA contamination occurred (C_t values were >40 cycles). No-template controls were also run in parallel on each plate. Transcript levels were derived from the accumulation of SYBR green fluorescence in a Light Cycler 480 (Roche, Meylan, France). The PCR conditions were as follows: 1× SYBR green mix (catalog no. 04707516001; Roche), 100 nmol l^{-1} primers and 1 µl of cDNA in a total volume of 20 µl. Each sample was run in triplicate. The dissociation curves showed a single amplification product and no primer dimer. Data were normalized using the $2^{-\Delta\Delta C_t}$ method (Livak and Schmittgen, 2001), where $-\Delta\Delta C_t=(C_{t\text{Target}}-C_{t\text{HKG}})_{t_x}-(C_{t\text{Target}}-C_{t\text{HKG}})_{t_0}$, t_x is the sampling time and t_0 is the incubation period starting point. Data are presented as fold changes in gene expression normalized to polyubiquitin transcript expression, as a housekeeping gene (HKG), and relative to gastrula stage control samples (pH_T 8.1). For each experiment, we checked that HKG expression was not affected by the experimental treatments and performed PCR on dilution of cDNA for both the target and the HKG to ensure that the efficiencies were similar.

Primer design and qRT-PCR

Primers for quantitative reverse transcriptase PCR (qRT-PCR) were developed using the *P. lividus* gene sequences *polyubiquitin* (AM596937.1), *msp130* (AM568814), *SM30* (AM569342.1), *Na^+/K^+-ATPase* subunits α (AM562805.1) and β (A554663.1) and fibroblast growth factor *fg9/16/20* (ABO65253). qRT-PCR primer sequences were designed using Primer3 software (http://frodo.wi.mit.edu/primer3/) to have a G+C content ranging from 50 to 60%. In addition, runs of three or more Cs or Gs at the 3′-ends of primers were avoided as they might have promoted mispriming at G- or C-rich sequences. Primers were chosen to generate equivalent amplicon lengths (Table 1). The melting temperature of the primers was set at 58°C. The qRT-PCR products were sequenced (VWR International, Fontenay-sous-Bois, France) and all matched the anticipated product. For each primer pair, the amplification efficiency (E) was determined on a 5-point 10-time dilution series of 100 ng cDNA extracted from all tested treatments to check for primer specificity. The amplification efficiencies were between 80 and 100% with a corresponding amplification factor between 1.8 and 2.0, respectively, for all primer combinations.

Data were analysed using N-way ANOVAs and Tukey's HSD multiple comparison tests were carried out to assess the significant differences between pH treatments.

In order to check whether differences between pH treatments were not only due to differences in developmental stages, gene expression was plotted against 'virtual age', which is an efficient way to correct for age when delayed larval development occurs (Pörtner et al., 2010). Virtual age corresponds to the time required for the larvae in controlled conditions to reach a precisely defined stage based on relevant morphometry. It was calculated from the inverse (exponential) transformation of the logarithmic relationship between larval overall length and time during the first 3 days at pH_T 8.1.

RESULTS

Culture conditions

The mean pH_T values from Day 0 to Day 3 are shown in Table 2. Mean temperature was 20.1±0.1°C (N=307) in both experiments. The mean A_T of FSW used during the experiment to fill the beakers was 2545±6 µmol kg^{-1}. It changed by 5 to 35 µmol kg^{-1} from Day 0 to Day 3 and averaged between 2550 and 2565 µmol kg^{-1} (mean A_T=2558 µmol kg^{-1}) depending on the culture conditions. P_{CO_2}

Table 2. Mean pH and carbonate chemistry of the treatments

Treatment	pH_T	P_{CO_2} (µatm)	DIC (µmol kg^{-1})	CO_3^{2-} (µmol kg^{-1})	Ω_c	Ω_a
Experiment A						
pH 7.0	6.97±0.03	6632±493	2734±18	24±2	0.57±0.04	0.37±0.03
pH 7.25	7.23±0.02	3555±209	2609±10	44±2	1.02±0.05	0.67±0.04
pH 7.5	7.48±0.03	1962±127	2515±10	74±4	1.74±0.10	1.13±0.06
pH 7.7	7.68±0.03	1188±77	2436±11	113±6	2.65±0.14	1.73±0.09
pH 7.9	7.86±0.04	743±84	2351±21	163±13	3.81±0.31	2.49±0.20
pH 8.1	8.08±0.01	397±13	2219±8	248±5	5.79±0.12	3.78±0.08
Experiment B						
pH 7.0	6.97±0.03	6590±461	2733±17	24±2	0.57±0.04	0.37±0.02
pH 7.25	7.22±0.03	3624±268	2612±13	43±3	1.00±0.07	0.65±0.04
pH 7.5	7.47±0.03	1996±149	2518±11	734±5	1.72±0.11	1.12±0.07
pH 7.7	7.69±0.02	1161±73	2432±10	115±6	2.70±0.13	1.76±0.09
pH 7.9	7.88±0.02	704±38	2341±11	169±7	3.95±0.16	2.58±0.10
pH 8.1	8.07±0.02	412±23	2227±13	243±9	5.68±0.20	3.70±0.13

Mean pH_T (on the total scale) values are calculated by transformation of pH_T to $[H^+]$ and reconversion of mean $[H^+]$ to pH_T. Partial pressure of CO_2 (P_{CO_2}), dissolved inorganic carbon (DIC), CO_3^{2-} concentration and saturation state of seawater with respect to calcite (Ω_c) and aragonite (Ω_a) are calculated from pH_T, temperature (20.1°C), salinity (38) and a mean total alkalinity (A_T) of 2558 µmol kg^{-1}. Data are means ± s.d. of measurements taken every 15 min from Day 0 to Day 3; N=307.

values and other parameters of the carbonate system were calculated using a mean A_T of 2558 µmol kg^{-1} and are given in Table 2.

Fertilization, survival and morphological development

The percentage of fertilization success was high (97–100%) in all treatments with no effect of pH in experiment A (one-way ANOVA, $F_{5,30}$=0.07, P=0.99) or experiment B ($F_{5,30}$=1.96, P=0.11) and no difference between experiments (t-test, t=0.78, P=0.44). The mean larval survival was also high and averaged 99 and 100% in experiments A and B, respectively. It did not vary between pH treatments in either experiment (one-way ANOVAs, P>0.05).

At 23 h post-fertilization, embryos were at the gastrula stage except in the pH_T 7.0 treatment, where only 35% of the embryos reached the early gastrula stage (the remaining 65% were at the blastula stage). At 46 h, the pluteus stage (4-arm stage) was completed in all treatments including pH_T 7.0.

The overall length of larvae from Day 2 to Day 3 (Fig. 1) was significantly affected by pH (two-way ANOVA, $F_{5,521}$=991.62, P<0.0001) and time ($F_{2,521}$=1083.28, P<0.0001), with a significant interaction between the two ($F_{10,521}$=3.42, P<0.001). Multiple comparison analyses revealed that larval length differed significantly between pH treatments (Tukey's HSD, P<0.0001), except between pH_T 8.1 and 7.9 and between pH_T 7.9 and 7.7 on Day 2 and between pH_T 8.1, 7.9 and 7.7 on Day 3 (Tukey's HSD, P>0.05). On Day 3, the overall length of larvae in the pH_T 7.5 treatment was 10% smaller than in the control treatment (pH_T 8.1), and it was 20 and 40% shorter in the pH_T 7.25 and 7.0 treatments, respectively, than in the control.

The symmetry index was high regardless of pH, with a mean ratio of the left to right overall length close to 1 (0.96–0.99). The index was significantly affected by pH (one-way ANOVA, $F_{5,174}$=3.76, P=0.003), with lower values at pH_T 7.25 and 7.0 than at pH_T 8.1, 7.9 and 7.5 (Tukey's HSD, P<0.05), but no difference between pH_T 7.7 and the other pH treatments (Tukey's HSD, P>0.05; Fig. 2).

Morphological analyses on Day 3 revealed that the length of arms was significantly affected by pH (one-way ANOVAs, P<0.0001; Tukey's HSD, post-oral arms: 8.1=7.9=7.7>7.5>7.25>7.0, antero-lateral arms: 8.1=7.9≥7.7>7.5>7.25>7.0; Fig. 3). Arms were 10–15% shorter at pH_T 7.5, 20–25% shorter at pH_T 7.25 and ~50% shorter at pH_T 7.0 relative to the control. The length of somatic rods was also affected by pH (one-way ANOVA, $F_{5,174}$=53.64, P<0.0001; Tukey's HSD, 8.1>7.9=7.7≥7.5>7.25=7.0); rods were 10% shorter at pH_T 7.9 and 7.7, 15% shorter at pH_T 7.5 and 30% shorter at pH_T 7.25 and 7.0 relative to the control. Larval width was not affected by pH, except at pH_T 7.0 where it was 10% smaller than in the other pH treatments (one-way ANOVA, $F_{5,174}$=144.79, P<0.0001; Tukey's HSD, 8.1=7.9=7.7=7.5=7.25>7.0). Allometric relationships between larval size (overall length) and the other morphometric parameters (Fig. 4) were similar in all pH treatments, except at pH_T 7.0 where significant differences in the intercepts were observed for somatic rod and post-oral arm length (ANCOVAs, P<0.0001).

The ratio of the post-oral arm to somatic rod length, which indicates the entrance of the larvae in the exotrophic phase (Bougis, 1971), was higher than 1 (1.1–1.2) in all treatments except at pH_T 7.0,

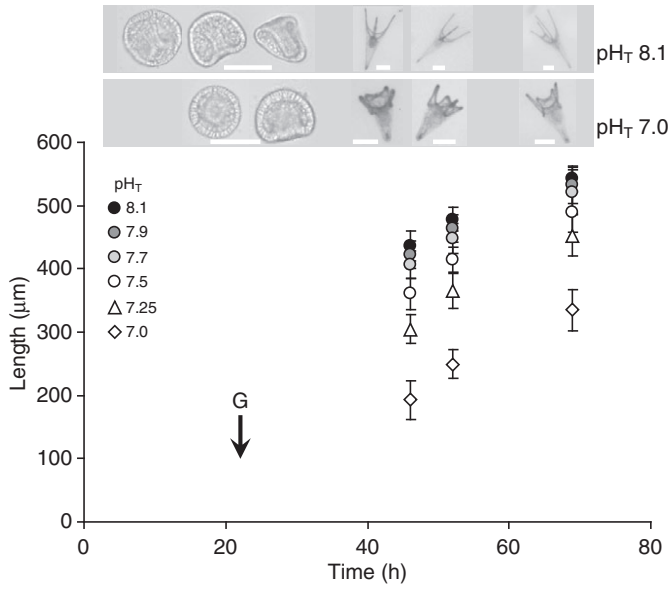

Fig. 1. *Paracentrotus lividus* larval overall length as a function of time in the different pH treatments at Day 2 (46 and 52 h post-fertilization) and Day 3 (69 h). The photographs correspond to the different sampling stages in the extreme pH treatments pH_T 7.0 and 8.1 (scale bars, 100 µm). G, gastrula stage (length, 100–120 µm). Data are means ± s.d.; N=30.

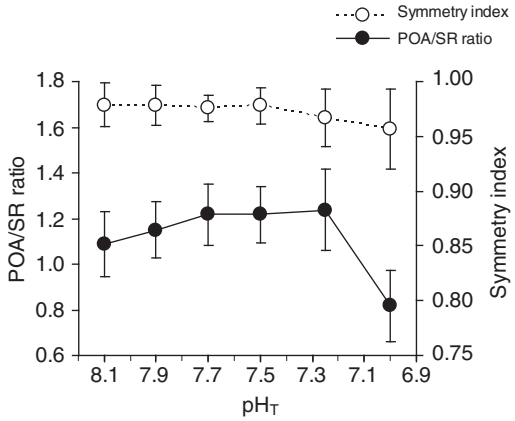

Fig. 2. Symmetry index and ratio of post-oral arm (POA) to somatic rod (SR) lengths in *P. lividus* in the different pH treatments. Data are means ± s.d.; *N*=30.

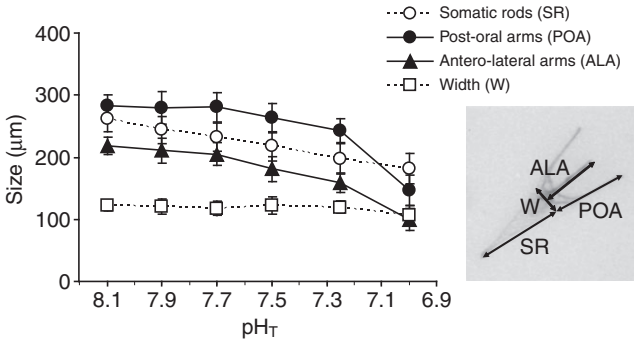

Fig. 3. *Paracentrotus lividus* larval width and lengths of somatic rods, post-oral arms and antero-lateral arms as a function of pH on Day 3. Data are means ± s.d.; *N*=30.

where it was 0.8 (one-way ANOVA, $F_{5,174}$=36.72, P<0.0001; Tukey's HSD, 7.25=7.5=7.7=7.9≥8.1>7.0; Fig. 2).

Ca incorporation

Passive ^{45}Ca adsorption on filters or larval tissues was negligible. Adsorption of ^{45}Ca on filters alone was not detectable after the successive rinsings with radiotracer-free seawater. The radioactivity measured on dead material was less than 0.1 Bq per filter (Q_{Ca}<0.01 nmol Ca larva^{-1}) after 44 h of exposure to FSW labelled with 50 kBq l^{-1} ^{45}Ca.

The incorporation of Ca in embryos remained close to zero during the first 24 h (Q_{Ca}≤0.01 nmol Ca individual^{-1}; Fig. 5A). Ca incorporation began at the gastrula stage on Day 1 (27 h post-fertilization) and increased linearly with time until Day 2 (53 h) at a rate of between 0.004 nmol Ca larva^{-1} h^{-1} at pH$_T$ 7.0 to 0.019 nmol Ca larva^{-1} h^{-1} at pH$_T$ 8.1 (linear regressions, R^2>0.96, P<0.0001), depending on pH, and then at a lower rate (from 0.004 nmol Ca larva^{-1} h^{-1} at pH$_T$ 7.0 to 0.009 nmol Ca larva^{-1} h^{-1} at pH$_T$ 7.9) until Day 3 (76 h). The rates of Ca incorporation from Day 1 (27 h) to Day 2 (53 h) differed significantly across pH treatments (ANCOVA, $F_{5,53}$=87.34, P<0.001; pairwise comparisons, 8.1=7.9>7.7>7.5>7.25>7.0). Ca incorporation was significantly correlated with pH at both the gastrula (r_S=0.97, P<0.0001) and four-arm stages (Days 2 and 3; r_S=0.91 to 0.98, P<0.0001). At the gastrula stage, Ca incorporation decreased linearly from pH$_T$ 8.1 to 7.0 at a rate of 0.06 nmol Ca gastrula^{-1} per pH unit (linear regression, R^2=0.96, P<0.0001). At the four-arm stage, it decreased at a rate of 0.3–0.4 nmol Ca larva^{-1} per pH unit (linear regressions, R^2=0.82 to 0.96, P<0.0001). Independently of pH, Q_{Ca} was highly correlated to the overall length (L) of larvae and followed an exponential function: Q_{Ca}=0.022e$^{0.0066L}$ (R^2=0.97, P<0.0001; Fig. 5B).

Gene expression

The molecular approach performed on genes of interest shows that their expression was systematically and significantly affected by either time or pH, with a significant interaction between both parameters (N-way ANOVA, P<0.05).

Genes involved in development

Transcripts related to *Na$^+$/K$^+$-ATPase* (α and β subunits) showed a similar expression pattern in organisms subjected to the ambient pH$_T$ of 8.1, with an increase in gene expression fold change in 52 to 69 h post-fertilization larvae. At lower pH$_T$ (7.9–7.25), the fold change in gene expression was increased compared with the control condition (pH$_T$ 8.1, 22 h post-fertilization), with a subsequent decrease at pH$_T$ 7.0. The highest variation in transcript expression was observed at pH$_T$ 7.25, with a gradual increase through larval development up to a 16.3±2.7- and 19.7±1.3-fold change in gene expression in 69 h post-fertilization larvae for α- and β-*Na$^+$/K$^+$ATPase*, respectively (Fig. 6A,B). Multiple comparison analyses (Tukey's HSD) revealed significant upregulation at pH$_T$≤7.5 in 22 h post-fertilization larvae, at pH$_T$≤7.25 in 46 h larvae and at pH$_T$ 7.25 in 52 and 69 h larvae (Fig. 6A). β-*Na$^+$/K$^+$-ATPase* transcript fold changes in expressions were already significantly upregulated at pH$_T$ 7.9 and 7.5 in the 46 and 52 h post-fertilization larvae, at pH$_T$ 7.5 in the 68 h larvae and at pH$_T$ 7.25 for all time points (Fig. 6B). At the extreme pH$_T$ of 7.0, the expression of α- and β-*Na$^+$/K$^+$-ATPase* suddenly stopped increasing and dropped to lower values, similar to the expression measured at pH$_T$ 8.1 for the β-subunit.

Genes involved in biomineralization

The fold change in the expression of transcripts coding for proteins involved in sea urchin biomineralization (*SM30*, *msp130* and *fg9/16/20*) was the highest in the pH$_T$ treatments ranging from 7.25 to 7.9. It decreased or was unchanged in the pH$_T$ 7.0 treatment (Fig. 7). Multiple comparison analyses (Tukey's HSD) applied to *fg9/16/20* revealed no regulation of expression by pH in 22 h post-fertilization larvae. The fold change in gene expression was then increased at pH$_T$ 7.9, 7.5 and 7.25 in 46 h larvae, only at pH$_T$ 7.5 and 7.25 in 52 h larvae and at all pH levels in 69 h larvae (Fig. 7A). The expression of the *msp130* transcript was significantly upregulated at pH$_T$<7.7 in 22 h larvae and only at pH$_T$ 7.5 in 46 h larvae. No significant variation was observed in subsequent larval stages (Fig. 7B). Finally, *SM30* transcript expression was not significantly changed in 22 h larvae but was upregulated at pH$_T$ 7.5 and 7.25 for the three subsequent larval stages, with a maximum of 25±3.8-, 23±1.6- and 23±3-fold changes in 46, 52 and 69 h larvae, respectively, at pH$_T$ 7.25 (Fig. 7C).

Gene expression and virtual age

According to the logarithmic relationship between overall larval length in the control group (L=272×ln$t$–610), the virtual age (h) was defined as VA=e$^{(L+610)/272}$. For example, larvae collected at pH$_T$ 7.5 at 46 h post-fertilization (real age) were smaller than in the

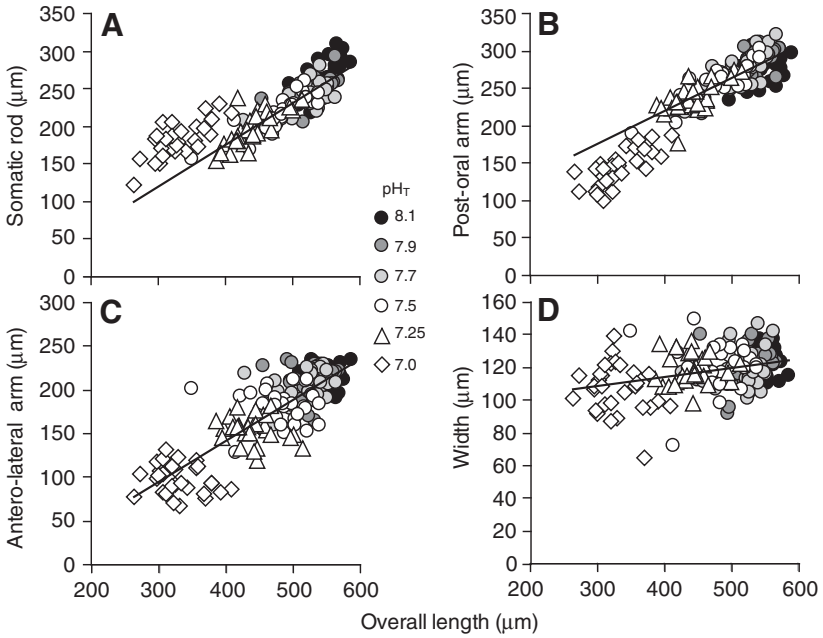

Fig. 4. Relationship between overall larval length and other morphometric parameters measured in *P. lividus* on Day 3 in the different pH treatments. (A) Somatic rod length; (B) post-oral arm length; (C) antero-lateral arm length; (D) larval width.

control treatment and corresponded to a virtual age of 36 h (delay in development of 10 h). When plotted against virtual age, two patterns of gene expression were observed in the control: (1) α- and β-*Na$^+$/K$^+$-ATPase* gene expression increased with time; and (2) *fg9/16/20*, *msp130* and *SM30* gene expression increased, reached a maximum at ~45 h and then decreased (Fig. 8). For all five tested genes, gene expression levels at pH$_T$ 7.9 and 7.7 were mostly within the range of control levels of expression, whereas in the lower pH treatments (pH$_T$<7.7), gene expression increased beyond the normal range of expression. However, it is interesting to note that for β-*Na$^+$/K$^+$-ATPase*, *fg9/16/20* and *msp130*, the expression at pH$_T$ 7.0 decreased and was within the levels observed in the control treatment.

DISCUSSION

Effect of pH on fertilization

The fertilization success of *P. lividus* was high (>97%) and was not affected by a decrease in pH. This broad tolerance to changes in pH is consistent with previous observations made for other species of sea urchin. Comparative data on the effects of decreased pH on sea urchin fertilization showed either no effect (Byrne et al., 2009a; Byrne et al., 2009b; Byrne et al., 2010) or an effect restricted to pH<7.4 (Bay et al., 1993; Kurihara and Shirayama, 2004). In *Heliocidaris erythrogramma*, fertilization success was similar in control and lower pH treatments (>90% from pH 7.9 to 7.6) (Byrne et al., 2009a). It dropped from ≥90% in controls to 70% at pH 7.4 in *Echinometra mathaei* (Kurihara and Shirayama, 2004) and to 60% at pH 7.0 in *Hemicentrotus pulcherrimus* and *Strongylocentrotus purpuratus* (Bay et al., 1993; Kurihara and Shirayama, 2004). In *P. lividus*, fertilization remained unaffected in the lowest pH treatments (pH$_T$ 7.25 and 7.0). The robustness of sea urchin fertilization to decreased pH is likely related to the low pH that is naturally associated with echinoderm reproduction, i.e. the low internal pH of activated sperm and the release of acid by eggs at fertilization (Byrne et al., 2009a). This suggests that sea urchin fertilization is highly tolerant to ocean acidification within the range of pH values projected in the next decades, or even below model predictions. However, because of favorable fertilization conditions in most laboratory experiments with no sperm-limiting conditions, fertilization success could be overestimated relative to natural systems. Recent studies revealed a 25% reduction in

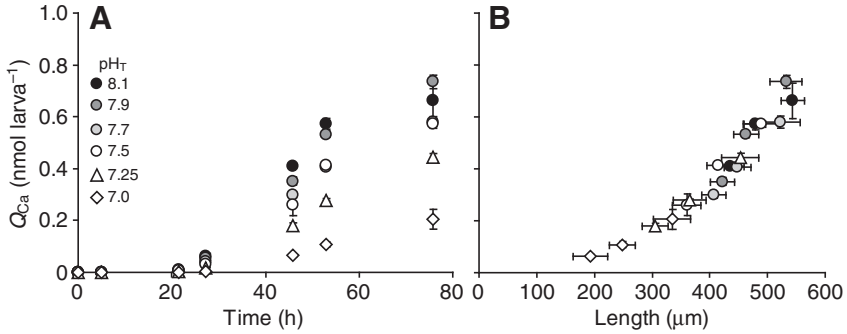

Fig. 5. (A) Calcium uptake with time in *P. lividus* embryos and larvae in the different pH treatments and (B) the relationship between calcium incorporation and overall length of larvae. Data are means ± s.d.; *N*=3 for calcium uptake and *N*=30 for larval overall length.

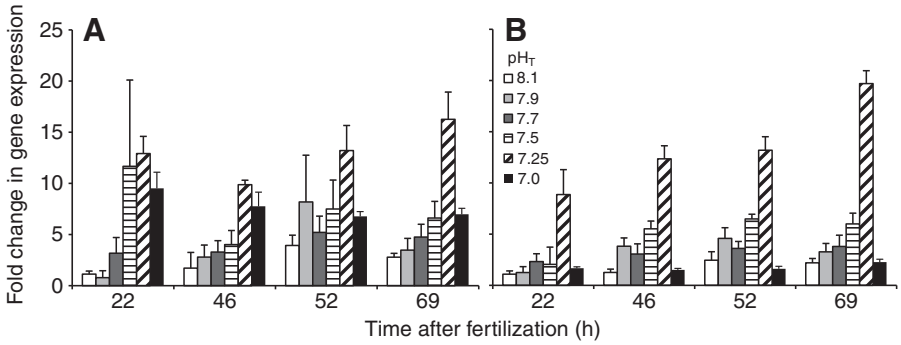

Fig. 6. Fold change in (A) α-*Na/KATPase* and (B) β-*Na/KATPase* expression in *P. lividus* in response to decreasing pH from pH$_T$ 8.1 (control) to pH$_T$ 7.0. Data are means ± s.d.; *N*=3.

fertilization success at pH 7.7 in *H. erythrogramma* (Havenhand et al., 2008) and a 72% drop in fertilization efficiency at pH 7.8 in *S. franciscanus* (Reuter et al., 2010), which may be attributed to decreased sperm motility.

Effect of pH on survival

The survival of *P. lividus* pluteus larvae in the present study was also high in the different pH treatments, with no significant differences between treatments. These results are consistent with those reported for the tropical (*Tripneustes gratilla*), temperate (*Pseudechinus huttoni*, *Evechinus chloroticus*) and polar (*Sterechinus neumayeri*) sea urchin species in which larval survival is unaffected until pH levels fall below 7.0 (Clark et al., 2009). However, although our results suggest that the pH values predicted to occur over the next 100–300 years will not directly affect the survival of *P. lividus* larvae, caution should be exercised in the interpretation of these results. Larval survival is reported only for the first 3 days of the larval stage, but prolonged exposure of plankton to elevated P_{CO_2} may have lethal effects (Yamada and Ikeda, 1999; Kikkawa et al., 2003) and it is possible that larvae may have been negatively affected after a longer period of time. For example, in the brittlestar *Ophiotrix fragilis*, larval survival is high during the first 3 days of culture at pH 7.7 and 7.9 but it drops to zero after 8 days under decreasing pH, relative to 70% for control larvae (Dupont et al., 2008). Further experiments are needed that consider the whole period of larval development in *P. lividus* for a better understanding of their survival in response to ocean acidification.

Effect of pH on development

An important delay in development was observed at pH$_T$ 7.0, where only 35% of embryos completed the gastrula stage 23 h post-fertilization relative to 100% at the other pH levels. The feeding stage of the pluteus larvae, characterized by a four-arm stage with a ratio of the post-oral arm to somatic rod length greater than 1 (Bougis, 1971), was also delayed in the pH$_T$ 7.0 treatment. At Day 3, it was not completed (ratio of 0.8), in contrast to pluteus larvae in the higher pH treatments (pH$_T$ 8.1 to 7.25), which had ratios of 1.1 to 1.2. The size of larvae at a given time post-fertilization was also affected at pH$_T$≤7.5, with a 10 to 40% reduction in overall length after 3 days of culture. The symmetry index, a good indicator of fitness (Dupont et al., 2008), was only slightly affected below pH$_T$ 7.25. With the exception of a small difference (5%) between the length of antero-lateral arms at pH$_T$ 8.1 and 7.7, arm length (post-oral and antero-lateral) was not significantly different among the pH$_T$ 8.1, 7.9 and 7.7 treatments, but was significantly reduced at pH$_T$≤7.5. Smaller size at the lowest pH levels could be explained either by a delay in development, a miniaturization of the larvae and/or phenotypic plasticity. However, allometries were observed between the overall length and the other morphometric parameters from pH$_T$ 8.1 to 7.25. Differences appeared only at pH$_T$ 7.0. These results strongly suggest that, down to a pH$_T$ of 7.25, the larvae at Day 3 have a normal morphology but are delayed in development. This is consistent with previous observations on the impact of low pH on larval development (Dupont et al., 2010c). More information on larval physiology is necessary to understand the origin of this delay, which could be related to a decrease (Pörtner and Farrell,

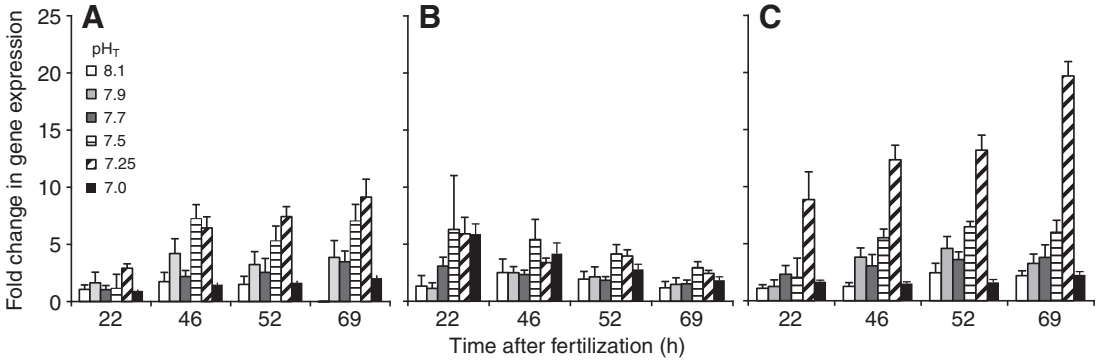

Fig. 7. Fold change in (A) *fg9/16/20*, (B) *msp130* and (C) *SM30* expression in *P. lividus* in response to decreasing pH from pH$_T$ 8.1 (control) to pH$_T$ 7.0. Data are means ± s.d.; *N*=3.

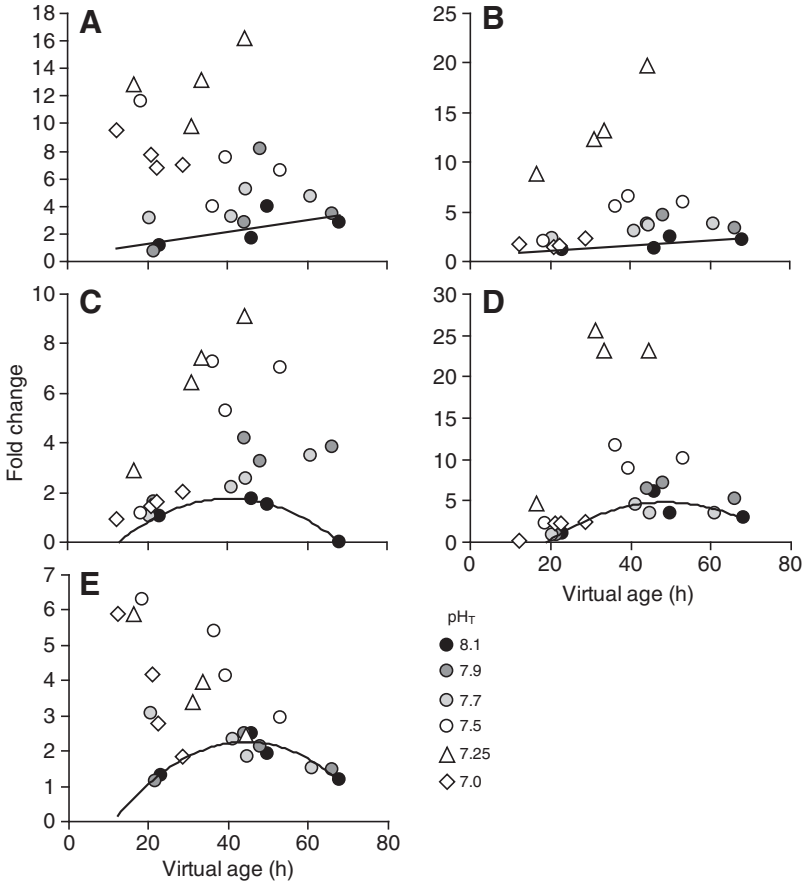

Fig. 8. Fold change in (A) α-*Na/KATPase*, (B) β-*Na/KATPase*, (C) *fg9/16/20*, (D) *msp130* and (E) *SM30* expression in *P. lividus* in response to decreasing pH from pH$_T$ 8.1 (control) to pH$_T$ 7.0 plotted against virtual age.

2008) or increase in metabolism associated with limited resources (Dupont et al., 2010a).

Effect of pH on calcification

The incorporation of Ca by the larvae was related to the formation of their skeleton. The larval skeleton is synthesized as a series of skeletal rods by the primary mesenchyme cells (PMCs) in the sea urchin embryo (Wilt, 2002). Ca incorporation in *P. lividus* was strongly related to time; it started at the embryonic stage and was the highest from the gastrula to the four-arm stage. It was also dependent on pH levels. At a given time post-fertilization, Ca incorporation decreased as a function of decreasing pH. Clark et al. (Clark et al., 2009) reported a 14–37% reduction in calcification index (percentage inorganic content of total dry weight) measured at pH 7.5–7.8 in larvae of several species of sea urchins. This is consistent with the difference observed in *P. lividus* at a given time (25–80%). However, independently of pH, calcium incorporation was strongly correlated with the overall larval length. Consequently, the apparent decrease in Ca incorporation is simply an indirect consequence of the impact of low pH on developmental rate. In other words, at a given developmental stage (or size), larvae present the same Ca incorporation rate regardless of pH.

Effect of pH at a molecular level

Development-related genes

The Na^+/K^+-ATPase enzymes targeted here drive most energy-dependent transport processes in sea urchins, and their total activity is a very significant metabolic component of development, accounting for 40% of the larval metabolic rate (Leong and Manahan, 1997). In the present study, the genes coding for the Na^+/K^+-ATPase heterodimer (α and β subunits) (Jorgensen and Skou, 1969) exhibited developmental regulation in the control treatment (pH$_T$ 8.1) with an increase in expression with time after fertilization. Comparative data have been obtained in the sea urchins *S. purpuratus* and *H. pulcherrimus*, where the expression of α-*Na^+/K^+-ATPase* gene increased rapidly during gastrulation (Mitsunaga-Nakatsubo et al., 1992). This latter expression pattern would suggest a subsequent increase in mRNA translation, producing a large increase in the sodium pump, presumably as a necessary component for proliferating cells. However, this hypothesis is rather speculative and needs to be confirmed by further analyses performed on Na^+/K^+-ATPase protein regulation in the sea urchin *P. lividus*.

Looking further into *P. lividus* molecular response to decreasing pH, we showed no significant change in the expression of *Na^+/K^+-ATPase* between the pH$_T$ 8.1 and 7.5 treatments through *P. lividus* early development (22 to 69 h post-fertilization). In contrast, a transcriptomic study performed on *S. purpuratus* larvae (early prism stage; 40 h post-fertilization) showed a decrease in *Na^+/K^+-ATPase* expression when pH decreased from 8.1 to 7.88 (Todgham and Hofmann, 2009). This discrepancy might be mainly due to a classic problem in developmental biology. The present study demonstrates that the expression of *Na^+/K^+-ATPase* genes increases with developmental time. Consequently, a slight delay in development will lead to an apparent downregulation of these genes (Pörtner et al., 2010). This is consistent with our results, which show no effect on gene expression in a similar range of pH when corrected by the developmental delay. However, the highest fold change in gene expression reported in this study, reaching up to 16- to 20-fold change at pH$_T$ 7.25 for α-*Na^+/K^+-ATPase* and β-*Na^+/K^+-ATPase*, respectively, cannot be explained by a delay

in development, and thus reflects a real impact of low pH on gene expression during early development. Finally, α-*Na*$^+$/*K*$^+$-*ATPase* transcript regulation was much lower once a certain P_{CO_2} value was surpassed (i.e. at pH_T 7.0), and this tendency was even stronger for the β-*Na*$^+$/*K*$^+$-*ATPase* subunit, for which expression remained unchanged compared with control conditions. This latter event might represent a potential energy-saving strategy in larval urchins, as it has been shown that acid/base regulations bear a significant cost. In the invertebrate *Sipunculus nudus*, the inhibition of both Na^+/H^+ exchange and Na^+-dependent Cl^-/HCO_3^- exchange and the predominant use of the more ATP-efficient carrier during extracellular acidosis contribute to the reduction in energy turnover that is reflected in a lower Na^+/K^+-ATPase activity (Pörtner et al., 2000). Comparable phenomena may also be involved in the protective effects of acidosis during anoxia in mammals (Bing et al., 1973; Pentilla and Trump, 1974; Bonventre and Cheung, 1985).

Calcification-related genes

We chose here among 100 protein candidates that have been recently identified as components of sea urchin tests and the spine organic matrix (Mann et al., 2008a; Mann et al., 2008b; Mann et al., 2010). Msp130 is a sulfated cell-surface glycoprotein that is thought to be involved in Ca uptake or precipitation (Carson et al., 1985; Leaf et al., 1987) and SM30 is an acidic glycoprotein of the spicule matrice (George et al., 1991).

In the present study, the transcripts *SM30* and *msp130* exhibited no significant variation in fold change in gene expression during the development of larvae grown at the control pH_T 8.1. However, when plotted against virtual age, the data showed a visible peak of expression at 46 h post-fertilization and a decrease through 69 h post-fertilization (Fig. 8). In the literature, a well-defined developmental regulation specific to both transcripts is described. Although the expression of *msp130* peaks in the early blastula stage and decreases through the pluteus stage, *SM30* mRNA accumulates later in development, appearing in the early gastrula through late pluteus stages (Guss and Ettensohn, 1997). Even though no significant difference in expression pattern was found in *msp130* and *SM30* at pH_T 8.1, gene regulation appeared highly dependent on pH and especially on developmental stage. Thus, although the fold change in the expression of *SM30* showed a significant response to decreasing pH in 46–69 h post-fertilization larvae at pH_T levels below 7.5, *msp130* expression only responded to decreasing pH in 22–46 h post-fertilization larvae at pH levels below 7.7. The lack of significant difference in the expression of *msp130* contrasts with the data obtained by Todgham and Hofmann (Todgham and Hofmann, 2009), which showed a decrease in expression in 40 h post-fertilization larvae from pH 7.96 to 7.88 (see comments on virtual age in Development-related genes).

Proteins related the fibroblast growth factor (*fg9/16/20*) transcripts are involved in PMC migration and skeletal morphology, prefiguring the branching pattern of the skeleton. The inhibition of the production of these transcripts has a dramatic effect on sea urchin biomineralization because it leads to the absence of skeleton (Röttinger et al., 2008). In the present study, the fold change in gene expression of *fg9/16/20* peaked at 46 h post-fertilization and decreased through 69 h post-fertilization larvae grown at pH_T 8.1. Röttinger et al. showed that the abundance of *fgfA* transcripts increased dramatically in mesenchyme gastrula of *P. lividus* and remained elevated from the onset of gastrulation up to the pluteus stage (48 h) (Röttinger et al., 2008).

In response to pH, we observed a gradual upregulation at all pH_T levels from 7.9 to 7.25, which could prevent the inhibition of calcification in the PMCs and/or $CaCO_3$ dissolution. However, once reaching the lowest pH_T of 7.0, the expression was significantly lower than that at pH_T 7.25 and was unchanged compared with the control treatment, also suggesting an energy-saving strategy. In fact, a pH_T of 7.0 corresponds to a highly undersaturated condition (see Ω_c and Ω_a values in Table 2). In such extreme conditions, leading to reduced deposition and $CaCO_3$ dissolution, the buffering of tissues can be made through calcite dissolution. Indeed, sea urchin larvae may be especially sensitive to acidosis. As osmoconformers they have a low capacity for ion regulation, which means they have a lesser ability to acid–base regulate through the process of ionic change used by many aquatic organisms (Pörtner, 2008; Clark et al., 2009). In this respect, at pH_T levels lower than 7.25, the cells might still try to cope with the effect of low pH, switching to other cellular metabolisms requiring vital energy.

Molecular plasticity

As a result of rapid and severe environmental changes expected for the near future, acclimation rather than adaptation is believed to be critical for short-term responses. The present study highlights substantial transcriptomic plasticity in larvae of the sea urchin *P. lividus* in response to a decline in pH in a short-term (3 day) experiment. In fact, fold change in gene expression gradually increased as a function of decreasing pH (pH_T>7.25) for the development and biomineralization genes investigated here. The transcription machinery here may act in a compensatory manner to preserve biological processes (e.g. biomineralization and development) under altered seawater chemistry of ocean acidification. However, at pH_T levels lower than 7.25, the physiological cost for cells to function in an altered environment might be too high. Wood et al. found that the brittle star *Amphiura filiformis* increased calcification and metabolism when exposed to reduced pH, but lost muscle mass as a consequence (Wood et al., 2008). Larvae from the red sea urchin *Strongylocentrotus franciscanus* raised under elevated CO_2 conditions and then subjected to a temperature shift revealed a reduced and delayed response in *hsp70* transcript level, a gene involved in the response to acute environmental stress, suggesting that physiological response may be impaired at the molecular level as a result of CO_2 exposure (O'Donnell et al., 2009). These results suggest that marine organisms may have the capacity to maintain protective mechanisms against ocean acidification, but this could come at a significant cost to an organism's ability to tolerate increased stress intensity (e.g. pH levels <7.5).

Molecular plasticity has been previously demonstrated among field populations of mollusks subject to environmental stress (Gracey et al., 2008; Place et al., 2008). In these larger-scale studies, which investigated a large part of the transcriptome, the regulation and modulation of gene expression appear as one of the most rapid and sensitive responses to environmental stresses and highlight a molecular strategy allowing life in fluctuating environments.

With regards to the early developmental stability of *P. lividus* larvae to decreasing pH reported here, we suggest that transcriptomic plasticity plays a major role in larval acclimation to ocean acidification, resulting in an optimistic scenario for sea urchin survival in acidifying seawater. In addition, the increasing amount of molecular data in both genomics (Sodergren et al., 2006) and proteomics (Mann et al., 2008a; Mann et al., 2008b) constitute a significant basis with which to promote the application of molecular approaches to multiple taxa in different geographic locations and thus identify further molecular targets involved in the early acclimation of sea urchin larvae to decreasing pH.

Conclusions

Our results suggest that the early developmental phases of the sea urchin *P. lividus* are relatively robust to predicted ocean acidification. Fertilization, larval survival, early development and calcification (up to 3 days) were not impacted by near-future ocean acidification (pH≥7.7, as projected by 2100). Previous investigations have already shown that the early development of sea urchins is only affected by pH values lower than 7.5 and is relatively insensitive to higher pH values (Kurihara and Shirayama, 2004; Byrne et al., 2009a). Surprisingly, early development of *P. lividus* also appeared to be resistant to a pH_T value of 7.0, with no effect on fertilization, Ca incorporation or survival. Parameters such as larval morphology and symmetry index were also unchanged down to pH_T 7.25 relative to a given developmental size and the only significant effect of pH was a delay in development. In other words, it takes more time and probably more energy (as suggested by the up to 20-fold increase in gene upregulation) to reach the same developmental stage. Morphology and fitness of *P. lividus* were only slightly affected at the extreme pH of 7.0, which can be considered a threshold for this species. This resistance to decreased pH is consistent with the wide distribution range and habitat (e.g. tidal pools) of this species. However, delay in development at lower pH levels may indirectly affect survival through increased mortality. The rates of larval mortality in the plankton are very high (Rumrill, 1990; Lamare and Barker, 1999) and any delay in the growth or development of larvae may mean that they are exposed to higher mortality for extended periods (Dupont et al., 2010b). We have also shown that the relative robustness in development is associated with a high molecular plasticity. The cost of such gene upregulation for the maintenance of growth and skeletal calcification and to what extent this cost may translate into later developmental stages is still unknown. However, this upregulation was not observed at the lowest pH (7.0) tested, suggesting an alternative mechanism or evidence of exhaustion that may lead to problems later in development.

ACKNOWLEDGEMENTS

We are grateful to D. Luquet, L. Gilletta and J.-Y. Carval for sea urchin sampling in the field. We thank T. Lepage for providing *P. lividus* transcript sequences and C. M. Moore for advice regarding statistics related to molecular data. The IAEA is grateful for the support provided to its Marine Environment Laboratories by the Government of the Principality of Monaco. S.D. is funded through the Linnaeus Centre for Marine Evolutionary Biology at the University of Gothenburg and supported by a Linnaeus grant from the Swedish Research Councils VR and Formas. This work is a contribution to the 'European Project on Ocean Acidification' (EPOCA), which received funding from the European Community's Seventh Framework Programme (FP7/2007-2013) under grant agreement no. 211384.

REFERENCES

Anthony, K. R., Kline, D. I., Diaz-Pulido, G., Dove, S. and Hoegh-Guldberg, O. (2008). Ocean acidification causes bleaching and productivity loss in coral reef builders. *Proc. Natl. Acad. Sci. USA* **105**, 17442-17446.

Bay, S., Burgess, R. and Nacci, D. (1993). Status and applications of echinoid (Phylum Echinodermata) toxicity test methods. In *Environmental Toxicology and Risk Assessment* (ed. W. G. Landis, J. S. Hughes and M. A. Lewis), pp. 281-302. Philadelphia, PA: American Society for Testing and Materials.

Berge, J. A., Bjerkeng, B., Pettersen, O., Schaanning, M. T. and Oxnevad, S. (2006). Effects of increased seawater concentrations of CO_2 on the growth of the bivalve *Mytilus edulis* L. *Chemosphere* **62**, 681-687.

Bing, O. H. L., Brooks, W. W. and Messer, J. V. (1973). Heart muscle viability following hypoxia: protective effects of acidosis. *Science* **180**, 1297-1298.

Bonventre, J. V. and Cheung, J. Y. (1985). Effects of metabolic acidosis on viability of cells exposed to anoxia. *Am. J. Physiol.* **249**, C149-C159.

Boudouresque, C. F. and Verlaque, M. (2001). Ecology of *Paracentrotus lividus*. In *Edible Sea Urchins: Biology and Ecology*, Vol. 32 (ed. J. M. Lawrence), pp. 177-216. Amsterdam: Elsevier Science.

Bougis, P. (1971). Effet de la température sur le développement endotrophe des plutéus. In *Fourth European Marine Biology Symposium* (ed. D. J. Crisp), pp. 197-201. Cambridge: Cambridge University Press.

Byrne, M., Ho, M., Selvakumaraswamy, P., Nguyen, H. D., Dworjanyn, S. A. and Davis, A. R. (2009a). Temperature, but not pH, compromises sea urchin fertilization and early development under near-future climate change scenarios. *Proc. R. Soc. B* **276**, 1883-1888.

Byrne, M., Soars, N., Selvakumaraswamy, P., Dworjanyn, S. A. and David, A. R. (2009b). Sea urchin fertilization in a warm, acidified and high pCO_2 ocean across a range of sperm densities. *Mar. Environ. Res.* **69**, 234-239.

Byrne, M., Soars, N. A., Ho, M. A., Wong, E., McElroy, D., Selvakumaraswamy, P., Dworjanyn, S. A. and Davis, A. R. (2010). Fertilization in a suite of coastal marine invertebrates from SE Australia is robust to near-future ocean warming and acidification. *Mar. Biol.* **157**, 2061-2069.

Caldeira, K. and Wickett, M. E. (2003). Anthropogenic carbon and ocean pH. *Nature* **425**, 365.

Caldeira, K. and Wickett, M. E. (2005). Ocean model predictions of chemistry changes from carbon dioxide emissions to the atmosphere and ocean. *J. Geophys. Res.* **110**, C09S04.

Carson, D. D., Farach, M. C., Earles, D. S., Decker, G. L. and Lennarz, W. J. (1985). A monoclonal antibody inhibits calcium accumulation and skeleton formation in cultured embryonic cells of the sea urchin. *Cell* **41**, 639-648.

Clark, D., Lamare, M. and Barber, M. (2009). Response of sea urchin pluteus larvae (Echinodermata: Echinoidea) to reduced seawater pH: a comparison among a tropical, temperate, and a polar species. *Mar. Biol.* **156**, 1125-1137.

Dickson, A. G. (2010). The carbon dioxide system in seawater: equilibrium chemistry and measurements. In *Guide to Best Practices for Ocean Acidification Research and Data Reporting* (ed. U. Riebesell, V. J. Fabry, L. Hansson and J.-P. Gattuso), pp. 17-40. Luxembourg: Publications Office of the European Union.

Dickson, A. G., Sabine, C. L. and Christian, J. R. (ed.) (2007). *Guide to Best Practices for Ocean CO_2 Measurements*, 191 pp. PICES Special Publication 3.

Dupont, S., Havenhand, J., Thorndyke, W., Peck, L. and Thorndyke, M. (2008). CO_2-driven ocean acidification radically affect larval survival and development in the brittlestar *Ophiothrix fragilis*. *Mar. Ecol. Prog. Ser.* **373**, 285-294.

Dupont, S., Lundve, B. and Thorndyke, M. (2010a). Near future ocean acidification increases growth rate of the lecithotrophic larvae and juvenile of the seastar *Crossaster papposus*. *J. Exp. Zool. Part B.* **314**, 382-359.

Dupont, S., Dorey, N. and Thorndyke, M. (2010b). What meta-analysis can tell us about vulnerability of marine biodiversity to ocean acidification? *Estuarine Coast. Shelf Sci.* **89**, 182-185.

Dupont, S., Ortega-Martinez, O. and Thorndyke, M. (2010c). Impact of near-future ocean acidification on echinoderms. *Ecotoxicology* **19**, 449-462.

Fenaux, L. (1968). Maturation de gonades et cycle saisonnier des larves chez *Arbacia lixula*, *Paracentrotus lividus* et *Psammechinus microtuberculatus* (Equinides) à Villefranche sur-Mer. *Vie Milieu* **19**, 1-52.

Fenaux, L., Etienne, M. and Quelart, G. (1987). Suivi écologique d'un peuplement de *Paracentrotus lividus* (Lamarck) dans la baie de Villefranche sur Mer. In *Colloque International sur Paracentrotus lividus et les Oursins Comestibles* (ed. C. F. Boudouresque), pp. 187-197. Marseille: GIS Posidonie Publication.

Gattuso, J.-P., Allemand, D. and Frankignoulle, M. (1999). Photosynthesis and calcification at cellular, organismal and community levels in coral reefs: a review on interactions and control by carbonate chemistry. *Am. Zool.* **39**, 160-183.

Gazeau, F., Quiblier, C., Jansen, J. M., Gattuso, J.-P., Middelburg, J. J. and Heip, C. H. R. (2007). Impact of elevated CO_2 on shellfish calcification. *Geophys. Res. Lett.* **34**, L07603.

George, N. C., Killian, C. E. and Wilt, F. H. (1991). Characterization and expression of a gene encoding a 30.6-kDa *Strongylocentrotus purpuratus* spicule matrix protein. *Dev. Biol.* **147**, 334-342.

Gooding, R. A., Harley, C. D. G. and Tang, E. (2009). Elevated water temperature and carbon dioxide concentration increase the growth of a keystone echinoderm. *Proc. Natl. Acad. Sci. USA* **106**, 9316-9321.

Gracey, A. Y., Chaney, M. L., Boomhower, J. P., Tyburczy, W. R., Connor, K. and Somero, G. N. (2008). Rhythms of gene expression in a fluctuating intertidal environment. *Curr. Biol.* **18**, 1501-1507.

Green, M. A., Jones, M. E., Boudreau, C. L., Moore, R. L. and Westman, B. A. (2004). Dissolution mortality of juvenile bivalves in coastal marine deposits. *Limnol. Oceanogr.* **49**, 727-734.

Guss, K. A. and Ettensohn, C. A. (1997). Skeletal morphogenesis in the sea urchin embryo: regulation of primary mesenchyme gene expression and skeletal rod growth by ectoderm-derived cues. *Development* **124**, 1899-1908.

Hamdoun, A. and Epel, D. (2007). Embryo stability and vulnerability in an always changing world. *Proc. Natl. Acad. Sci. USA* **104**, 1745-1750.

Havenhand, J. N., Buttler, F.-R., Thorndyke, M. C. and Williamson, J. E. (2008). Near-future levels of ocean acidification reduce fertilization success in a sea urchin. *Curr. Biol.* **18**, 651-652.

Jorgensen, P. L. and Skou, J. C. (1969). Preparation of highly active Na^+,K^+-ATPase from the outer medulla of rabbit kidney. *Biochem. Biophys. Res. Commun.* **37**, 39-47.

Kikkawa, T., Ishimatsu, A. and Kita, J. (2003). Acute CO_2 tolerance during the early developmental stages of four marine teleosts. *Environ. Toxicol.* **18**, 375-382.

Kurihara, H. and Shirayama, Y. (2004). Effects of increased atmospheric CO_2 on sea urchin early development. *Mar. Ecol. Prog. Ser.* **274**, 161-169.

Kurihara, H., Kato, S. and Ishimatsu, A. (2007). Effect of increased seawater pCO_2 on early development of the oyster *Crassostrea gigas*. *Aquat. Biol.* **1**, 91-98.

Lamare, M. D. and Barker, M. F. (1999). *In situ* estimates of larval development and mortality in the New Zealand sea urchin *Evechinus chloroticus* (Echinodermata: Echinoidea). *Mar. Ecol. Prog. Ser.* **180**, 197-211.

Lavigne, H. and Gattuso, J.-P. (2010). Seacarb: seawater carbonate chemistry with R. R package version 2.3.3. http://cran.r-project.org/web/packages/seacarb/index.html

Leaf, D. S., Anstrom, J. A., Chin, J. E., Harkey, M. A., Showman, R. M. and Raff, R. A. (1987). Antibodies to a fusion protein identify a cDNA clone encoding msp130, a primary mesenchyme-specific cell surface protein of the sea urchin embryo. *Dev. Biol.* **121**, 29-40.

Leong, P. K. K. and Manahan, D. T. (1997). Metabolic importance of Na^+/K^+-ATPase activity during sea urchin development. *J. Exp. Biol.* **200**, 2881-2892.

Livak, K. J. and Schmittgen, T. D. (2001). Analysis of relative gene expression data using real-time quantitative PCR and the $2^{-\Delta\Delta C_T}$ method. *Methods* **25**, 402-408.
Mann, K., Poustka, A. J. and Mann, M. (2008a). The sea urchin (*Strongylocentrotus purpuratus*) test and spine proteomes. *Proteome Sci.* **6**, 22.
Mann, K., Poustka, A. J. and Mann, M. (2008b). In depth, high-accuracy proteomics of sea urchin tooth organic matrix. *Proteome Sci.* **6**, 33.
Mann, K., Wilt, F. H. and Poustka, A. J. (2010). Proteomic analysis of sea urchin (*Strongylocentrotus purpuratus*) spicule matrix. *Proteome Sci.* **17**, 8-33.
McEdward, L. R. and Miner, B. G. (2007). Echinoid larval ecology. In *Edible Sea Urchins: Biology and Ecology*, 2nd edn (ed. J. M. Lawrence), pp. 71-93. Amsterdam: Elsevier.
Miles, H., Widdicombe, S., Spicer, J. I. and Hall-Spencer, J. (2007). Effects of anthropogenic seawater acidification on acid-base balance in the sea urchin *Psammechinus miliaris*. *Mar. Pollut. Bull.* **54**, 89-96.
Mitsunaga-Nakatsubo, K., Fujiwara, A. and Yasumasu, I. (1992). Change in the activity of Na+,K+-ATPase in embryos of the sea urchin, *Hemicentrotus pulcherrimus*, during early development. *Dev. Growth Differ.* **34**, 379-385.
Morse, J. W., Arvidson, R. S. and Lüttge, A. (2007). Calcium carbonate formation and dissolution. *Chem. Rev.* **107**, 342-381.
O'Donnell, M. J., Todgham, A. E., Sewell, M. A., Hammond, L. M., Ruggiero, K., Fangue, N. A., Zippay, M. L. and Hofmann, G. E. (2010). Ocean acidification alters skeletogenesis and gene expression in larval sea urchins. *Mar. Ecol. Prog. Ser.* **398**, 157-171.
Orr, J. C., Fabry, V. J., Aumont, O., Bopp, L. D., Diney, S. C., Feely, R. A., Gnanadesikan, A., Gruber, N., Ishida, A., Joos, F. et al. (2005). Anthropogenic ocean acidification over the twenty-first century and its impact on calcifying organisms. *Nature* **437**, 681-686.
Pedrotti, M. L. and Fenaux, L. (1992). Dispersal of echinoderm larvae in a geographic area marked by an upwelling (Ligurian Sea, NW Mediterranean). *Mar. Ecol. Prog. Ser.* **86**, 117-127.
Pedrotti, M. L. and Fenaux, L. (1993). Effects of food diet on the survival, development and growth rates of two cultured echinoplutei (*Paracentrotus lividus* and *Arbacia lixula*). *Int. J. invertebr. Reprod. Dev.* **24**, 59-70.
Pentilla, A. and Trump, B. F. (1974). Extracellular acidosis protects Ehrlich ascites tumor cells and rat renal cortex against anoxic injury. *Science* **185**, 277-278.
Place, S. P., O'Donnell, M. J. and Hofmann, G. E. (2008). Gene expression in the intertidal mussel *Mytilus californianus*: physiological response to environmental factors on a biogeographic scale. *Mar. Ecol. Prog. Ser.* **356**, 1-14.
Pörtner, H. O. (2008). Ecosystem effects of ocean acidification in times of ocean warming: a physiologist's view. *Mar. Ecol. Prog. Ser.* **373**, 203-217.
Pörtner, H. O. and Farrell, A. P. (2008). Ecology. Physiology and climate change. *Science* **322**, 690-692.
Pörtner, H. O., Bock, C. and Reipschläger, A. (2000). Modulation of the cost of pHi regulation during metabolic depression: a (31)P-NMR study in invertebrate (*Sipunculus nudus*) isolated muscle. *J. Exp. Biol.* **203**, 2417-2428.
Pörtner, H. O., Dupont, S., Melzner, F. and Thorndyke, M. (2010). Laboratory experiments and benthic mesocosm studies. In *Guide to Best Practices for Ocean Acidification Research and Data Reporting* (ed. U. Riebesell, V. J. Fabry, L. Hansson and J.-P. Gattuso), pp. 167-180. Luxembourg: Publications Office of the European Union.
Raven, J., Caldeira, K., Elderfield, H., Hough-Guldberg, O., Liss, P., Riebesell, U., Shepherd, J., Turley, C. M. and Watson, A. (2005). *Ocean Acidification due to Increasing Atmospheric Carbon Dioxide. Policy document 12/05*. London: The Royal Society.
Reuter, K. E., Lotterhos, K. E., Crim, R. N., Thompson, C. A. and Harley, C. D. G. (2010). Elevated pCO_2 increases sperm limitation and risk of polyspermy in the red sea urchin *Strongylocentrotus franciscanus*. *Glob. Change Biol.* **17**, 163-171.
Röttinger, E., Saudemont, A., Duboc, V., Besnardeau, L., McClay, D. and Lepage, T. (2008). FGF signals guide migration of mesenchymal cells, control skeletal morphogenesis and regulate gastrulation during sea urchin development. *Development* **135**, 353-365.
Rumrill, S. S. (1990). Natural mortality of marine invertebrate larvae. *Ophelia* **32**, 163-198.
Shirayama, Y. and Thornton, H. (2005). Effect of increased atmospheric CO_2 on shallow water marine benthos. *J. Geophys. Res.* **110**, C09S08.
Sodergren, E., Weinstock, G. M., Davidson, E. H., Cameron, R. A., Gibbs, R. A., Angerer, R. C., Angerer, L. M., Arnone, M. I., Burgess, D. R., Burke, R. D. et al. (2006). The genome of the sea urchin *Strongylocentrotus purpuratus*. *Science* **314**, 941-952.
Solomon, S., Qin, D., Manning, Z., Chen, Z., Marquis, M., Averyt, K. B., Tignor, M. and Miller, H. L. (2007). *Climate Change 2007, the Physical Science Basis. Contribution of Working Group I to the Fourth Assessment Report of the Intergovernmental Panel on Climate Change*. Cambridge: Cambridge University Press.
Suwa, R., Nakamura, M., Morita, M., Shimada, K., Iguchi, A., Sakai, K. and Suzuki, A. (2010). Effects of acidified seawater on early life stages of scleractinian corals (Genus Acropora). *Fish. Sci.* **76**, 93-99.
Todgham, A. E. and Hofmann, G. E. (2009). Transcriptomic response of sea urchin larvae *Strongylocentrotus purpuratus* to CO_2-driven seawater acidification. *J. Exp. Biol.* **212**, 2579-2594.
Turley, C., Findlay, H. S., Mangi, S., Ridgwell, A. and Schmidt, D. N. (2009). CO_2 and ocean acidification. In *Marine Climate Change Ecosystem Linkages Report Card 2009* (ed. J. M. Baxter, P. J. Buckley and M. T. Frost), Online science reviews, 25 pp. www.mccip.org.uk/elr/acidification.
Wilt, F. H. (2002). Review, biomineralization of the spicules of sea urchin embryos. *Zool. Sci.* **19**, 253-261.
Wood, H. L., Spicer, J. I. and Widdiecombe, S. (2008). Ocean acidification may increase calcification rates, but at a cost. *Proc. R. Soc. B* **275**, 1767-1773.
Yamada, Y. and Ikeda, T. (1999). Acute toxicity of lowered pH to some oceanic zooplankton. *Plankton Biol. Ecol.* **46**, 62-67.